

Alkali-metal segregation at glass surfaces during electron irradiation

A. Miotello

Dipartimento di Fisica, Università Degli Studi di Trento, I-38050 Povo Trento, Italy

G. Cinque, P. Mazzoldi, and C. G. Pantano*

Dipartimento di Fisica, Università Degli Studi di Padova, I-35100 Padova, Italy

(Received 27 July 1990; revised manuscript received 28 September 1990)

It is shown that Gibbsian segregation is an important feature of the redistribution of alkali metal in the surface of glass during electron irradiation. A model that couples the effects of segregation, desorption, and diffusion is presented. The model is used to simulate the alkali-metal ion desorption flux, and both the ion-scattering- and Auger-electron-spectroscopy signal changes, which have been experimentally measured.

I. INTRODUCTION

During the electron irradiation of glasses, the local surface concentration and depth distribution of alkali-metal species can change. This redistribution is of concern in the analysis of glass surfaces using techniques such as electron microprobe analysis (EMP) and Auger-electron spectroscopy (AES), and in the use of glasses in electron emission devices such as single-channel electron multipliers and microchannel plate detectors. Indeed, there have been many studies of this redistribution—both experimental and theoretical. The experimental studies have relied, largely, on the measurements of Auger-electron signal changes during continuous electron irradiation, while the theoretical studies have focused predominantly on the electric-field-enhanced migration and electron-beam-enhanced desorption of alkali metal. In general, the theoretical models have succeeded in simulating the Auger-electron signal decay that has been measured under various conditions of electron irradiation and in many different glasses. But in those cases where monolayer-sensitive techniques such as ion scattering spectroscopy (ISS) or desorption spectroscopy have been used to measure the change of alkali-metal surface concentration, an initial increase of the alkali-metal signal has been observed. The purpose of this paper is to discuss the possible origins of this increase and to show that it can only be explained and simulated through an electron-bombardment-enhanced Gibbsian segregation of alkali metal.

II. BACKGROUND

It is now well established that the electron irradiation of alkali-metal-containing silicate glasses causes a change in the surface composition.¹⁻⁴ This is mainly due to the creation of an electric field within the glass surface over the penetration range of the incident electrons. The primary effect is the electromigration of the alkali-metal species towards the bulk of the material. This electron-beam effect has been extensively studied with Auger-electron spectroscopy and with nuclear reaction analy-

ses.¹⁻⁴ A continuity equation that couples the effects of ordinary and field-assisted diffusion describes, quite well, the kinetics of the signal change observed in the AES and nuclear-reaction analysis (NRA).⁵ These techniques measure the average signal change over depth scales where the primary effect is a net decrease in the sodium concentration and/or signal. Figure 1 shows, for example, the excellent fit between the Auger signal decay and the signal decay calculated on the basis of an ordinary diffusion of alkali metal.⁶

Nevertheless it must be emphasized that there also exists an electron-stimulated desorption of alkali metal during electron irradiation and this, too, will influence the measured surface composition and signal decay.^{7,8} Figure

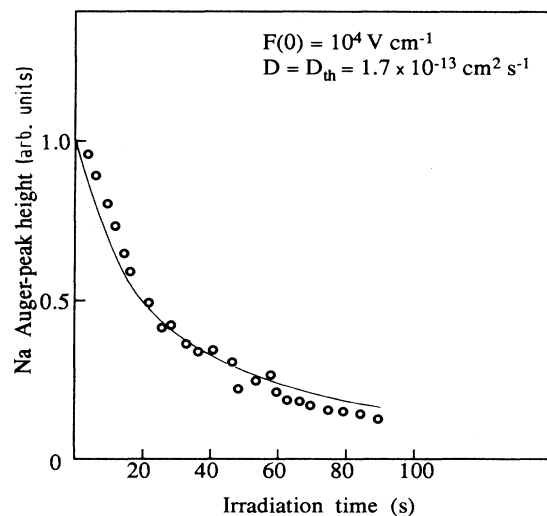


FIG. 1. Experimental results (open points) taken from Ref. 8 and the calculated profile (Ref. 6) for the Na Auger peak heights from soda-silicate glass under electron irradiation at room temperature. The theoretical profile has been obtained with a value of the electrical field at the surface $F(0) = -\nabla\phi|_{x=0}$ as reported in the figure and an alkali-metal diffusion coefficient D coincident with the ordinary diffusion coefficient D_{th} .

2 presents experimental evidence of the electron-stimulated desorption of sodium that was reported by Ohuchi and Holloway.⁸ In their theoretical simulation of the Auger-electron signal decay and the desorption flux, where an initial increase is observed, a model based upon ionization, desorption, and diffusion was necessary to fit the data.⁸ The ionization of the alkali metal to a non-bonded state was required to explain the initial increase in the desorption flux, but in general there is no direct experimental support for this ionization in the case of alkali metal in glass. It can also be seen in Fig. 1 of Ref. 8 (solid lines) that their model does not fit the data very well at short times where the increase is most dramatic.

More recently, ion scattering spectroscopy was used by Then and Pantano⁹ to follow the alkali-metal concentration evolution in the surface of glass during electron irradiation. This measurement is most sensitive to the alkali-metal behavior in the surface monolayer and, as shown in Fig. 3, an initial increase of the cesium concentration is observed. ISS measurements on other glasses showed initial increases of Rb and K as well. These investigators suggested that the initial increase in the alkali-metal concentration could be due to the electric-field-driven out-migration in the outermost 2–3 atomic layers of the glass. In this regard it is significant that Cazaux¹⁰ has proposed the existence of an inversion point in the electron-beam-induced surface electric field that could provide a driving force for this out-migration process.

We have considered in more detail the possible effects of an inversion point in the electric field according to the Cazaux model. It is not difficult to prove that the Cazaux model does not succeed in explaining the ISS results through the presence of an inversion point. Indeed, according to the general model of Ref. 11, where Poisson's equation, with appropriate boundary conditions, has been numerically solved to compute the actual distribution of charged species in an electron-irradiated glass (for typical experimental conditions), it has been proven that the to-

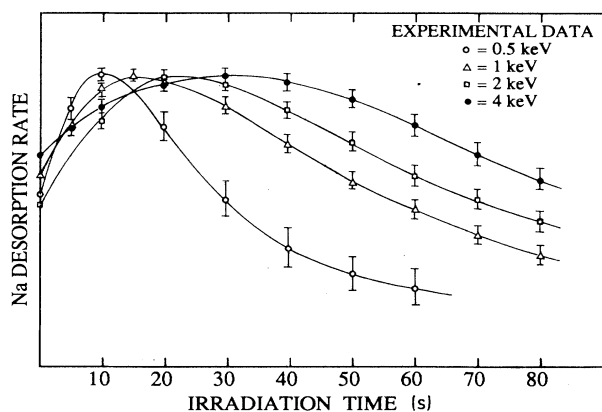


FIG. 2. Experimental desorption rate of Na (from soda-silica glass) as a function of electron-irradiation time at different primary electron energies (Ref. 8) (the solid lines are drawn only to guide the eyes).

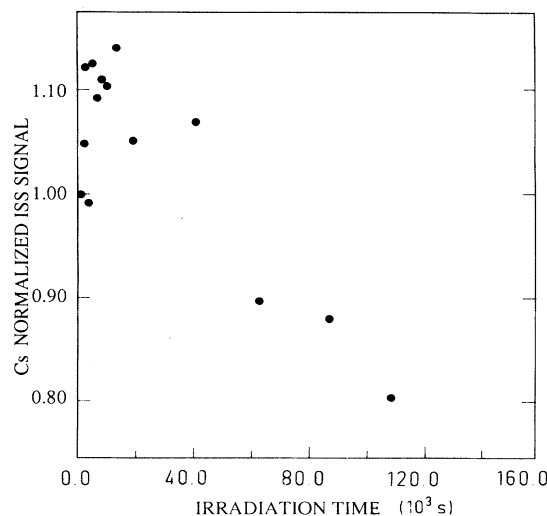


FIG. 3. Cs normalized ISS signal as a function of electron-irradiation time (electron energy $E=500$ eV, current density $=5 \mu\text{A cm}^{-2}$) from Cs-Rb lead silicate glass (Ref. 9).

tal number of both positive and negative charges must be nearly the same, otherwise dielectric breakdown phenomena occur. This means that the in-depth coordinate of the inversion point is expected to be almost zero (surface position): i.e., no inversion point exists. Moreover, the existence of an inversion point is questionable also on the basis of known experimental data regarding AES measurements on glasses. Indeed, Cazaux tried to explain the experimental results of Gossink *et al.*,³ in particular the time evolution of Ca (increase) and Na (decrease) looking at the inelastic mean free path λ of Auger electrons of the migrating ions as compared to the inversion point position. Notice that the Cazaux model fails to work if we look at the experimental K and Ca AES signals evolution reported in Fig. 7 of Ref. 3. Indeed, the λ parameter is essentially the same (LMM Auger transition) for both species, while their behavior is opposite. Such a peculiar phenomenon was explained in terms of correlation effects occurring between the migrating species (Na-Ca and K-Ca) when their concentration into the glass is greater than or equal to 0.1 (molar fraction).¹²

Altogether, it should be clear that an increase in the monolayer surface concentration of alkali metal can occur under electron-beam irradiation. This can be detected in desorption measurements and in ion scattering analysis during the initial stages of electron bombardment, but it is not detected using Auger analysis. This effect—that is, the increase—cannot be explained on the basis of an electric-field-induced out-diffusion.

Here, it is proposed that there exists a driving force for the Gibbsian segregation of alkali-metal species to the surface monolayer of the glass. This segregation is enhanced during electron (and probably ion) irradiation. The segregation can be detected during the initial stage of the irradiation using monolayer-sensitive techniques such as ISS or desorption, but not in AES due to the averaging effects over the Auger-electron escape depth. The segre-

gation effect—that is, the increased surface concentration—is not observed in the later stages of the irradiation due to the depletion of alkali metal in the surface region through desorption and in-diffusion. All of these effects are coupled because the surface concentration determines the driving force for the desorption and the diffusion. Thus, the net change in the surface concentration and the desorption flux can only be explained using a model that includes all of these processes (segregation, desorption, and diffusion). And to explain the differences in signal behavior detected in ISS and AES, the depth sensitivity of the analysis techniques must be included. After a brief discussion of segregation effects in glass, a computer simulation of these coupled phenomena and their effects upon ISS and AES signal changes during electron irradiation will be presented.

III. SURFACE SEGREGATION IN GLASSES

Does a thermodynamic or other basis exist to presuppose the possible Gibbsian segregation of alkali metal to the surface of silicate glasses? In the case of metal alloys, where the existence of ion-bombardment-induced segregation has been aptly demonstrated by Kelly,¹³ equilibrium segregation effects were already well founded. In fact, a wide database existed to compare the extent of bombardment-induced segregation with the associated thermodynamic driving force for segregation. No such database exists to support the thermodynamics of segregation in glasses because they are essentially nonequilibrium states of matter. The fact that most glasses of interest are covalently bonded materials creates more difficulty in the theoretical description of segregation. Nevertheless, it can be argued that in the case of multicomponent silicate glasses, especially those modified with alkali metal and/or alkaline earth species, the chemical binding forces intrinsic to the glass structure itself strongly suggest fundamental driving forces for segregation. The structure of alkali metal and alkaline earth silicate glasses is based upon an infinite silica network that is decorated with the weakly bound alkali-metal (alkaline) ions.¹⁴ The network is strong and covalently bonded, while the modifier species are bound through ionic bonds. The surface of this glass, especially the clean surface created through fracture or ion sputtering in vacuum, consists of SiO_4 tetrahedra that can bear a net negative charge. This charge could, in principle, be shielded through the segregation of alkali-metal species in the surface monolayer. Moreover the polarizability of the alkali-metal (alkaline) ions, especially those of large ionic radius such as K, Rb, or Cs, would further reduce the energy of these surfaces. The reported data on surface tension of molten glasses support this hypothesis, i.e., the surface tension of $\text{K}_2\text{O-SiO}_2$, is less than $\text{Na}_2\text{O-SiO}_2$ and in both cases the tension decreases with an increasing concentration of alkali metal.¹⁴ In recent years, the nature of clean glasses surfaces—that is, surfaces created by fracture in vacuum—has been reported.^{14,15} Their direct analysis (without any significant amount of electron or ion bombardment) reveals that the surface concentration of alkali metal is enhanced relative to the bulk. In the case where

ion scattering spectroscopy was used due to its monolayer surface sensitivity (here with exceedingly low doses of He scattering), an almost complete Na or K monolayer was observed for binary sodium-silicate and potassium-silicate glasses, respectively. A molecular-dynamics simulation has also been performed to characterize the clean surface of alkali-metal silicate glass.¹⁶ The results showed the accumulation of alkali-metal in the outermost 0.2–0.3 nm of the surface, and not surprisingly, an alkali-metal-depleted region in the subsurface. Due to the kinetic limitations at room temperature, this redistribution of alkali-metal is confined to only the first and second layers; i.e., it does not represent the state of equilibrium segregation. Nevertheless, it reveals the tendency for alkali-metal segregation at room temperature, even in the absence of any significant bombardment. In light of these findings, it comes as no surprise that electron (and ion) bombardment of alkali-metal silicate glasses—which already possess defective structures—would be exceedingly susceptible to bombardment-induced segregation.

IV. THE MODEL

In this section let us briefly discuss the transport equations through which we describe the experimental results concerning the surface behavior of alkali-metal species in electron-irradiated glasses as detected by ISS and ion desorption measurements. It is well known that electron irradiation of a dielectric causes the formation of an electric field whose structure was extensively discussed in Ref. 11. The driving force due to the gradient of the electrochemical potential $\mu^* = \mu - q\phi$ (here, μ is the chemical potential, q is the charge, and ϕ is the electric potential) induces an ionic flux given by

$$\mathbf{J} = -D\nabla n + \mu_e n \nabla \phi \quad (1)$$

and then the continuity equation for the charge-carrier concentrations $n = n(x, t)$ at time t and depth x ($x = 0$ is the surface position) is

$$\frac{\partial n}{\partial t} = \nabla \cdot (D\nabla n) - \mu_e \nabla \cdot (n \nabla \phi) . \quad (2)$$

D is the ordinary diffusion coefficient and μ_e is the mobility connected to D by the Nernst-Einstein equation. Equation (2) simply describes bulk ionic fluxes due to electrochemical gradients. To include the possible surface effects of segregation we must consider some new boundary conditions. Specifically, we describe the time evolution of alkali-metal concentration $\Gamma(t)$ just on the surface, due to Gibbsian segregation, through the relation

$$\frac{d\Gamma(t)}{dt} = v_G n . \quad (3)$$

In Eq. (3) n is the concentration (function of time) of ions in subsurface layer and v_G is an “effective” velocity connected to the jumping process (due to Gibbsian segregation) of ions from subsurface layer to the top layer (from where desorption occurs). As we shall see, we are able to reproduce both the experimental ISS and alkali-metal desorption results by using a constant value (as electron irradiation proceeds) for v_G ; its actual value is only con-

nected to the different kinds of alkali-metal ions or to the atomic glass composition.

Equation (3) is a simple effective approach to describe surface Gibbsian segregation in glass but at this stage we have no other choice since the physical aspects of a glass surface are not clarified at all, mainly under irradiation conditions. In particular, many processes, such as chemical bond breaking, long interval times involved in electronic deexcitation, desorption processes promoted by electronic excitation, etc., may influence the physical state of the glass surface, under irradiation, and also the physical processes leading the system to the ground state. However since in glasses under irradiation condition the ionic transport is stimulated,⁴ the kinetic of alkali-metal segregation is expected to be more pronounced with respect to the ordinary conditions (i.e., without irradiation).

Now, coming back to Eq. (3), notice that without such a condition the alkali-metal surface concentration may only exhibit a decreasing behavior during irradiation since the driving force associated with the electric field is directed towards the interior of the glass.

As to the alkali-metal desorption process, we include it in our computation scheme through the "evaporation law:"

$$-D\nabla n|_{x=0} + \mu_E n \nabla \phi|_{x=0} + v_G n|_{x=0} = \Delta x_0 \sigma J_e n|_{x=0}, \quad (4)$$

which stems from a balance between alkali-metal fluxes just at the surface. In Eq. (4) σ is the alkali-metal desorption cross section, J_e is the flux of impinging particles causing desorption, while Δx_0 is the thickness of the surface layer from which desorption may occur (Δx_0 ranges between 0.3 and 0.5 mm). In Eqs. (1)–(4) both the transport parameters and the σ coefficients are unknown from previous experiments even if their order of magnitude may be deduced from the literature concerning irradiation effects in glasses.⁴ In any case, we have chosen to treat the above-mentioned quantities as well as v_G as free parameters in the computational scheme. General analytical solutions of Eqs. (1)–(4) are not available and there is no straightforward method for fitting these equations to the experimental data. We used an empirical trial-and-error procedure for fitting the experimental results, obtaining the values of transport parameters reported in Table I, II, and III.

V. SIMULATION OF THE ISS SIGNAL

In Fig. 4 we report, along with the ISS experimental results for Rb and Cs of the electron-irradiated Rb-Cs lead silicate glasses, the theoretical profiles obtained by numerical integration of Eqs. (1)–(4). The obtained values for the transport and σ parameters are summarized in Table I. The structure of the electric field as a function of the depth is linear, the maximum value being at the surface as discussed in Ref. 12. The obtained transport parameters for Rb and Cs are not very different among them. The diffusion coefficient turns out to be of the order of $(2-5) \times 10^{-20}$ cm²/sec, a value that should be

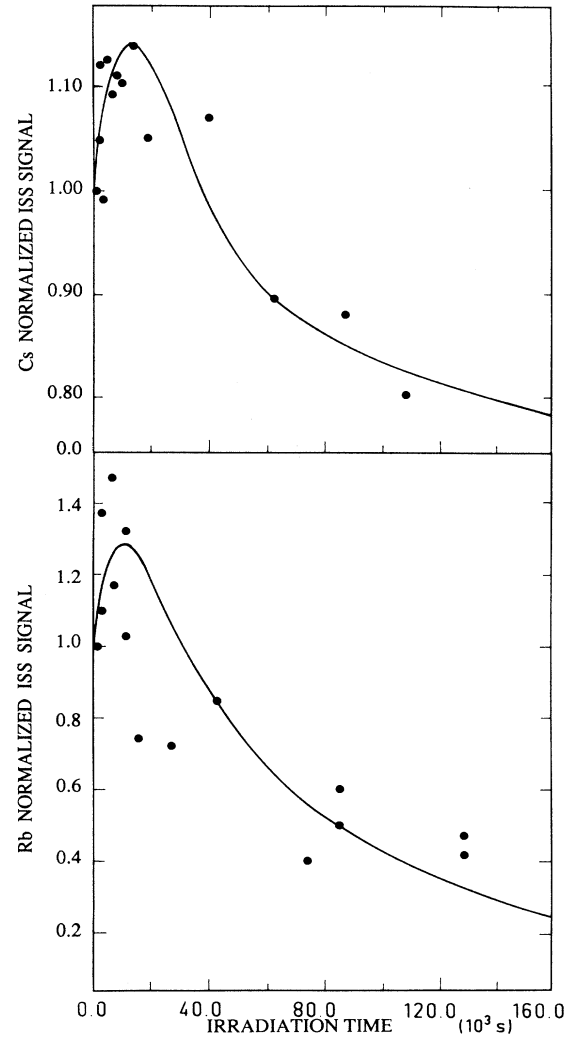


FIG. 4. Experimental (Ref. 9) Rb and Cs (Rb-Cs lead silicate glass) normalized ISS signals (solid points) as a function of electron-irradiation time ($E = 500$ eV, current density $= 5 \mu\text{A cm}^{-2}$). The solid lines have been obtained by the numerical integration of Eqs. (1)–(4) (see text).

compared to the known value of 1.8×10^{-19} cm²/sec of Na in a glass of composition $20\text{Na}_2\text{O}-10\text{PbO}-70\text{SiO}_2$, at room temperature.¹⁷ As opposed to the transport parameters, the σ values are quite different, even if this difference may be associated with the large dispersion of the experimental points at the initial stage of the electron irradiation. In Fig. 5 we report along with ISS experi-

TABLE I. Actual parameters used in Eqs. (1)–(4) to fit the experimental ISS results for Rb-Cs lead silicate (Ref. 9) glass.

D (cm ² s ⁻¹)	v_G (cm s ⁻¹)	σ (cm ²)	$-\Delta\phi _{x=0}$ (V cm ⁻¹)	
2×10^{-20}	1.1×10^{-11}	2.6×10^{-19}	2.6×10^6	Rb
5×10^{-20}	4.4×10^{-12}	3.2×10^{-20}	2.6×10^6	Cs

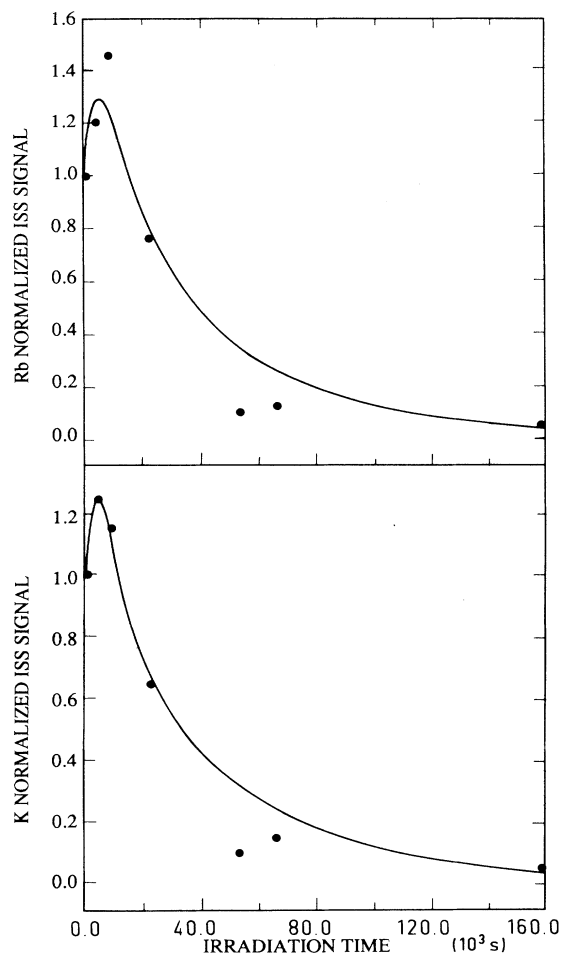


FIG. 5. Experimental (Ref. 9) Rb and K (Rb-K lead silicate glass) normalized ISS signals (solid points) as a function of electron-irradiation time ($E=500$ eV, current density= $5 \mu\text{A cm}^{-2}$). The solid lines have been obtained by the numerical integration of Eqs. (1)–(4) (see text).

mental Rb and K (solid points) results of the electron-irradiated Rb-K lead silicate glass, the theoretical profiles obtained by numerical integration of Eqs. (1)–(4). The obtained values for the transport and σ parameters are summarized in Table II. It is important to note that both in Rb-K and Rb-Cs lead silicate glasses, the Rb alkali-metal exhibits the same behavior.

VI. SIMULATION OF DESORPTION FLUX

For our purpose, the ISS experiments are equivalent to the desorption experiments since in both cases the “ex-

TABLE II. Actual parameters used in Eqs. (1)–(4) to fit the experimental ISS results for K-Rb lead silicate glass (Ref. 9).

D ($\text{cm}^2 \text{s}^{-1}$)	v_G (cm s^{-1})	σ (cm^2)	$-\nabla\phi _{x=0}$ (V cm^{-1})	
2×10^{-20}	1.2×10^{-11}	6.4×10^{-19}	2.6×10^6	Rb
5×10^{-20}	1.3×10^{-11}	6.4×10^{-19}	2.6×10^6	K

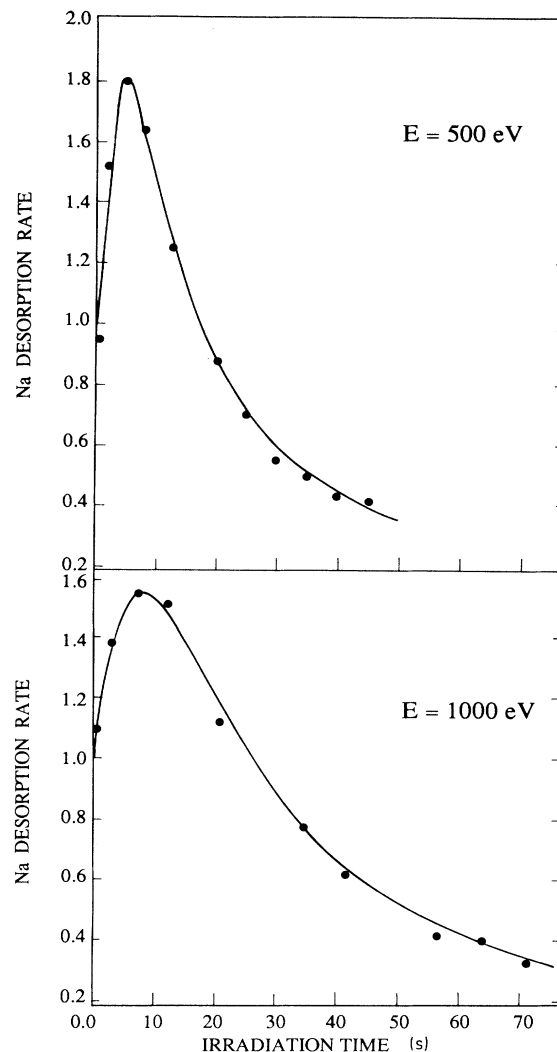


FIG. 6. Normalized Na desorption rate as function of electron-irradiation time in soda-silicate glass at two different E values (current density= 2 mA cm^{-2}). The points are the experimental data from Ref. 7 and the solid curves have been obtained by the numerical integration of Eqs. (1)–(4) (see also the text).

perimental signal” is proportional to the surface alkali-metal concentration. In Fig. 6 we report along with the experimental desorption data (solid points) as obtained by irradiation of a $\text{Na}_2\text{O-SiO}_2$ glass⁷ with primary electrons having energy E , respectively, of 500 and 1000 eV, the

TABLE III. Actual parameters used in Eqs. (1)–(4) to fit the experimental desorption data (Ref. 7) for e -irradiated soda silicate glass.

D ($\text{cm}^2 \text{s}^{-1}$)	v_G (cm s^{-1})	σ (cm^2)	$-\nabla\phi _{x=0}$ (V cm^{-1})	E eV
5×10^{-15}	2.9×10^{-8}	6.75×10^{-18}	4.4×10^4	1000
4×10^{-15}	4×10^{-8}	1.3×10^{-17}	5.2×10^4	500

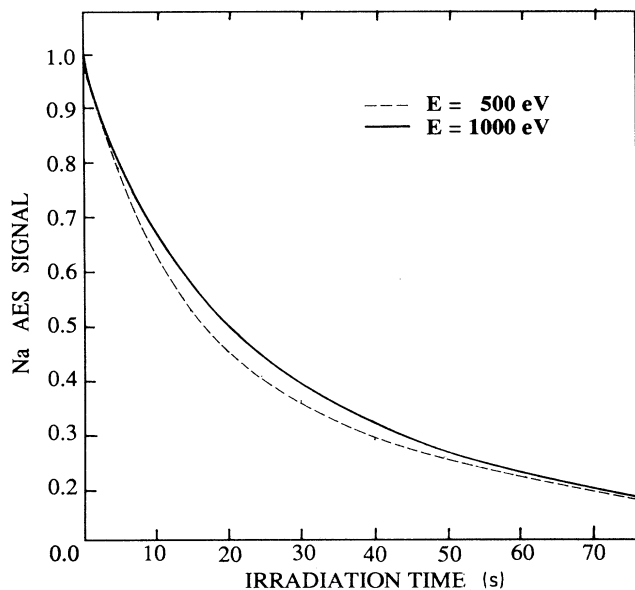


FIG. 7. Calculated AES signals (normalized) corresponding to the surface concentration evolution of Fig. 6; note that even in the case where Gibbsian segregation is accounted for, only an Auger signal decrease is observed (see also Fig. 7 of Ref. 8).

theoretical profiles computed through numerical integration of Eqs. (1)–(4). In Table III we report the values of the relevant parameters employed in the computation to obtain a good fit of the experimental results. Notice that all parameters have essentially the same values both for 500- and 1000-eV e -irradiation, the only relevant difference being connected to the σ parameter: this fact, however, may be understood looking at the experimental results of Wang *et al.*¹⁸ reporting an increase of σ for Na in electron-irradiated $\text{Na}_2\text{O}-2\text{SiO}_2$ as a function of primary electron energy when Si $2p$ and O $1s$ electronic levels are ionized.

VII. SIMULATION OF AES SIGNAL

In Fig. 7 we report the computed AES signals of Na pertinent to the Na profiles evolution under the surface of the e -irradiated glasses of the previous figure. A mean free path¹⁹ of Auger electrons, $\lambda = 2.8$ nm, was employed in the calculation. Only a decreasing behavior of the AES signal is evident, confirming that the AES technique is not too useful to study atomic composition in the top layer of a solid.

VIII. SUMMARY

It has been shown that the initial increase in alkali-metal surface concentration that occurs during electron irradiation of glass surfaces can be explained on the basis of Gibbsian segregation. We suggest that the effect is analogous to the ion-bombardment-induced segregation effect observed during the sputtering of metal alloys and compounds. It was also shown that the surface concentration increase due to Gibbsian segregation of alkali-metal ions is only seen using monolayer-sensitive techniques (ISS and ESD) even if it may also influence the corresponding Auger signal decrease. In the vacuum environments where ESD and sputtering are of interest, the segregation effect is especially significant because equilibrium can never be achieved; i.e., segregation provides a driving force for the transport of species to the surface where the desorption occurs within an infinite chemical potential gradient (the vacuum). The only reason there is an apparent steady state in the desorption flux, or equivalently the surface concentration, is the depletion zone that forms beneath the surface.

ACKNOWLEDGMENTS

We would like to thank Dr. Roger Kelly of IBM (New York) for useful discussions on the interpretation of the ISS and ESD results. One of the authors (G.C.) acknowledges the Istituto per la Ricerca Scientifica e Tecnologica (Trento) for financial support.

*Permanent address: Department of Materials Science and Engineering, Pennsylvania State University, University Park, PA 16802.

¹C. G. Pantano, D. B. Dove, and G. Y. Onoda, *J. Vac. Sci. Technol.* **13**, 414 (1976).

²F. Ohuchi, M. Ogino, P. H. Holloway, and C. G. Pantano, *Surf. Interf. Anal.* **2**, 85 (1980).

³R. G. Gossink, H. Van Doveren, and J. A. T. Verhoeven, *J. Non-Cryst. Solids* **37**, 111 (1980).

⁴P. Mazzoldi and A. Miotello, *Radiat. Eff.* **98**, 39 (1986).

⁵A. Miotello and P. Mazzoldi, *J. Phys. C* **15**, 5615 (1982).

⁶A. Miotello, *J. Phys. C* **19**, 445 (1986).

⁷F. Ohuchi and P. H. Holloway, *Scanning Electron. Microsc.* **4**, 1453 (1982).

⁸F. Ohuchi and P. H. Holloway, *J. Vac. Sci. Technol.* **20**, 863 (1982).

⁹A. M. Then and C. G. Pantano, *J. Non-Cryst. Solids* **120**, 178 (1990).

¹⁰J. Cazaux, *J. Appl. Phys.* **59**, 1418 (1986).

¹¹A. Miotello, *Phys. Lett.* **103A**, 279 (1984); *J. Phys. C* **19**, L201 (1986).

¹²A. Miotello and P. Mazzoldi, *Phys. Rev. Lett.* **54**, 1675 (1985).

¹³R. Kelly, *Mater. Sci. Eng. A* **115**, 11 (1989), and references quoted therein.

¹⁴W. D. Kingery, H. K. Bowen, and D. R. Uhlmann *Introduction to Ceramics*, 2nd ed. (Wiley, New York, 1976).

¹⁵J. P. Lacharme, P. Champion, and D. Leger, *Scanning Electron. Microsc.* **1**, 237 (1981).

¹⁶J. F. Kelso, C. G. Pantano, and S. H. Garofolini, *Surf. Sci.* **134**, L543 (1983).

¹⁷G. H. Frischat, *Ionic Diffusion in Oxide Glasses* (Trans Tech, Bay Village, OH, 1976).

¹⁸Y. X. Wang, F. Ohuchi, and P. H. Holloway, *J. Vac. Sci. Technol. A* **2**, 732 (1984).

¹⁹M. P. Seah and W. A. Dench, *Surf. Interf. Anal.* **1**, 2 (1979).